Am J Transl Res 2025;17(9):7468-7481
www.ajtr.org /ISSN:1943-8141/AJTR0167325

Original Article

Study on drug sensitivity and clinical application of tumor organoid-based colorectal cancer models

Yiwang Hu, Junchang Zhu, Yinjie Zheng, Jinyuan Zhang, Kai Yang, Yifei Pan

Department of Colorectal and Anal Surgery, The First Affiliated Hospital of Wenzhou Medical University, Nanbaixiang Campus, Wenzhou 325000, Zhejiang, China

Received July 9, 2025; Accepted September 3, 2025; Epub September 15, 2025; Published September 30, 2025

Abstract: Objectives: To establish and validate a patient-derived organoid (PDO) model of colorectal cancer (CRC) for drug sensitivity testing and assess its correlation with clinical treatment outcomes. Methods: Tumor tissues were collected from 16 CRC patients undergoing surgery. PDOs were successfully generated from 9 cases and exposed to five chemotherapeutic agents (5-FU, oxaliplatin, irinotecan, raltitrexed, trifluridine) and one targeted therapy (cetuximab). IC50 values (half-maximal inhibitory concentration) and inhibition rates were determined and compared with patients' clinical responses. Results: PDOs displayed heterogeneity in drug sensitivity. RAS-mutant organoids were consistently resistant to cetuximab, whereas RAS wild-type organoids showed variable responses. In most cases, PDO drug responses correlated with clinical treatment outcomes, suggesting that the PDO model can accurately reflect individual therapeutic sensitivity. Conclusions: CRC PDOs can be efficiently established and serve as reliable in vitro models for predicting responses to chemotherapy and targeted therapies. This approach may guide personalized treatment strategies and improve clinical decision-making in CRC.

Keywords: Colorectal cancer, organoids, drug sensitivity, precision medicine, cetuximab, RAS mutation

Introduction

Colorectal cancer (CRC) is one of the most common malignant tumors worldwide, ranking third in incidence and second in mortality. In 2020, there were an estimated 1.9 million new cases and over 930,000 deaths from CRC [1]. Although advances in surgical techniques, imaging, and early screening have significantly improved prognosis, systemic therapy remains essential for CRC treatment [2]. Chemotherapy regimens, such as 5-fluorouracil (5-FU), oxaliplatin, and irinotecan, often combined with targeted therapies like cetuximab, are the standard treatment [3]. However, FOLFIRI (leucovorin, fluorouracil, and irinotecan) and FOLFOX (leucovorin, fluorouracil, and oxaliplatin) achieve only a 50% objective response rate [4, 5]. Furthermore, nearly all patients who initially respond to treatment eventually develop drug resistance. Clinically, many patients do not respond well to the first-line treatment, leading to tumor progression after the initial course. This delays optimal treatment timing, impacts the patient's health, increases fear of chemotherapy, and complicates subsequent treatments. Therefore, the development of precision models to predict drug efficacy in CRC patients is urgent.

Traditional research methods for studying tumor drug sensitivity often yield unsatisfactory results. Conventional 2D cell line cultures are widely used, but they lack the cell-cell interactions and microenvironment necessary to simulate in vivo conditions, and cannot accurately replicate the three-dimensional structure of tumors. Additionally, genetic variation during cell passaging can affect the reliability of drug efficacy assessments [6]. The microtumor patient-derived tumor-like cell cluster (PTC) model optimizes the culture medium and microenvironment for primary cells, enabling personalized drug testing within two weeks of obtaining tumor samples [7]. However, long-term cultivation of PTCs is challenging, and drug response patterns can change after four weeks, potentially due to the loss of stromal cells. While PTCs are closer to real tumors than traditional cell lines, they still fail to capture all the cellular het-

https://doi.org/10.62347/WUEG2637

erogeneity and cannot model immunotherapy or angiogenesis-based treatments due to the absence of T cells and endothelial cells. Patient-Derived Xenografts (PDX) models, which retain many characteristics and the microenvironment of the original tumor, are valuable but time-consuming, expensive, and have a low success rate, which can delay treatment and hinder their application in precision medicine [8].

Patient-Derived Organoids (PDOs) are an advanced in vitro model that better represents the genomic and histopathological features of tumors [9]. PDOs are 3D cultures that retain key properties of the organs they mimic, including self-renewing stem cells that differentiate into multiple organ-specific cell types, spatial organization, and functional characteristics. These models provide a physiologically relevant system for drug testing. PDOs can be derived from tissue samples containing adult stem cells, single adult stem cells, or organoids from pluripotent stem cells. They maintain the structure, morphology, genetic mutations, and heterogeneity of the original tumor and are widely used to model various cancers, including CRC, gastric cancer, lung cancer, pancreatic cancer, liver cancer, breast cancer, and prostate cancer [10]. Studies have shown that organoids derived from metastatic CRC can predict chemotherapy responses [11], but targeted drug therapies have not been extensively studied.

This study aims to establish a CRC PDO model, assess drug sensitivity to commonly used chemotherapeutic agents (5-FU, oxaliplatin, irinotecan) and targeted therapies (cetuximab), and compare the drug responses with clinical treatment outcomes. IC50 values will be determined for these drugs, and the dose-response relationship will be analyzed to evaluate the model's predictive value. It is hypothesized that the PDO model can accurately reflect a patient's drug response, thereby providing a reliable tool for predicting individualized treatment efficacy and supporting personalized treatment strategies for CRC patients.

Methods

Study design

This study aimed to construct a PDO model of CRC and evaluate its sensitivity to chemotherapy and targeted therapy drugs.

Setting

This prospective study was conducted at the First Affiliated Hospital of Wenzhou Medical University, with a total of 16 CRC samples collected from September 2022 to September 2023. Data collection, exposure, and follow-up took place during this period, including postoperative assessments and quarterly telephone follow-ups. Treatment plans and imaging results were recorded. Disease progression or relapse was assessed by experienced oncologists and radiologists based on imaging until July 31, 2024. The follow-up period was set to end on this date, ensuring a minimum of 10 months of follow-up for all patients, with tumor recurrence or progression evaluated every 3 months through imaging.

Participants

Inclusion criteria: 1) Aged 18-75 years; 2) Histologically confirmed adenocarcinoma in the descending colon, sigmoid colon, or upper rectum (≥ 10 cm from the anal verge), based on colonoscopy and biopsy; 3) Availability of surgically resected tumor tissue, with at least one specimen ≥ 1 cm in diameter; tissue collection did not interfere with pathological diagnosis or clinical treatment; 4) Preoperative imaging indicating stage III or IV disease with lymph node or distant metastasis, according to the AJCC staging system; 5) No prior chemotherapy, radiotherapy, or targeted therapy before surgery.

Exclusion criteria: 1) Patients with metastatic lesions only and no resectable primary tumors; 2) Incomplete clinical data (e.g., missing ethnicity, age, or tumor differentiation grade); 3) Concurrent diagnosis of other malignancies; 4) Life expectancy less than 1 month at the time of inclusion.

Clinical and pathological data were extracted from the hospital's electronic medical record system, including CT and MRI imaging and postoperative follow-up. All procedures adhered to the Declaration of Helsinki (December revision), and written informed consent was obtained from all participants for tissue collection and research use.

Variables

Key outcome variables included the drug sensitivity of PDOs to chemotherapy and targeted

drugs, assessed by IC50 values and inhibition rates at blood drug concentrations. Secondary variables included patient demographics, tumor stage, and genetic mutations.

Data sources/measurement

Preparation of the reagents: The basic medium was prepared by mixing 465 mL Advanced DMEM/F12, 25 mL L-glutamine (200 mM), 5 mL HEPES (1 M), and 5 mL penicillin/streptomycin mixture, and stored at 4°C. The HISC medium was prepared by adding 2 mL B-27 (50X), 1 μM N-acetylcysteine, 10 mM nicotinamide, 10 nM gastrin I, 100 μM A83-01, 300 μM SB202190, 10 mM prostaglandin E2, and 0.2 mL Primocin. The digestion medium was made by mixing 10 mL DMEM, 500 U/mL collagenase IV, 1.5 mg/mL collagenase II, 20 mg/mL hyaluronidase, 0.1 mg/mL dispase II, 10 μM Y-27632, and 1% fetal bovine serum. The growth factor-containing matrix gel was prepared by adding 1 μg RSPO-1, 0.5 μg Noggin, and 0.5 μg EGFR to 1 mL Matrigel. The organoid wash buffer was PBS containing 100 μg/mL Primocin and 0.1% BSA. The matrix gel was thawed overnight at 4°C before use.

Tissue sampling by CRC organization: Immediately following surgical removal, tissue samples were placed in organoid cleaning solution and basic culture medium pre-chilled at 4°C to ensure sample viability. Tissue sampling occurred within 10 minutes of isolation. Necrotic tissue and fat were removed in the operating room, and samples were washed three times for 5 minutes each in organoid cleaning solution. The samples were then immersed in basic culture medium, stored in an ice box with an ice pack, and transported to the laboratory within 24 hours. The remaining colorectal cancer tissue was divided into cryogenic tubes, preserved in RNA preservation solution, and transferred to a -80°C freezer or liquid nitrogen for long-term storage. Basic clinical information about the patient was recorded.

Processing specimens and obtaining isolated cells: Tissue was cut into 1-3 mm^2 pieces in a sterile petri dish on ice, then placed in ice-cold PBS with penicillin/streptomycin and shaken for 5 minutes, repeated 5 times. The sample was transferred to a 15 mL centrifuge tube, and 8 mL digestion solution was added. The mixture was incubated at 37°C in a shaker at 120 rpm for 1 hour, with shaking every 15 minutes until the suspension was homogeneous. The suspension was filtered, and centrifuged at 4°C and 300 g for 5 minutes. The supernatant was discarded, and the cell pellet was resuspended in 6 mL of basic medium and centrifuged again. If red blood cells were present, the pellet was treated with red blood cell lysis solution, then resuspended and centrifuged. The washing process was repeated three times to obtain a single-cell suspension. After counting, the cell suspension was adjusted to a density of 20,000 cells per well. The cells were resuspended in 40 μL of Matrigel per well, mixed gently, and seeded into 24-well plates. The Matrigel-cell mixture was allowed to solidify at 37°C for 30 minutes before adding culture medium. Subsequently, 500 μL of pre-warmed HISC medium was added to each well, and the organoids were cultured in a 37°C, 5% CO_2 incubator.

Organoid drug sensitivity test: Well-grown organoids were seeded at a density of 200 organoids per well in a 48-well plate, with 100 μL of basic medium added to each well. The plate was placed in a 37°C cell culture incubator for incubation. Drugs were added after 3-4 days of culture. Chemotherapeutic agents and targeted drugs commonly used in CRC treatment were selected, with DMSO as the blank control. Drug concentrations were prepared in the following gradients: 100, 10, 1, 0.1, 0.01, 0.001, and 0.0001 μM for 5-FU, irinotecan, oxaliplatin, trifluridine, and raltitrexed. For cetuximab, concentrations of 5×10^{-2}, 5×10^{-3}, 5×10^{-4}, 5×10^{-5}, 5×10^{-6}, 5×10^{-7}, and 5×10^{-8} M were used. Each drug concentration had no fewer than three replicates. After 72 hours of drug exposure, cell viability was assessed using an ATP-based luminescence assay kit (CellTiter-Glo® Luminescent Cell Viability Assay, Promega, USA), according to the manufacturer's instructions. Briefly, after 72 hours of drug exposure, the culture medium was removed, and organoids were incubated with an equal volume of ATP assay reagent for 10 minutes at room temperature with gentle shaking. This induced cell lysis and stabilized the luminescent signal. Luminescence intensity, which is directly proportional to intracellular ATP levels and thus to viable cell numbers, was measured using a microplate reader (BioTek Synergy H1).

Each condition was tested in triplicate, and background signals from blank controls were subtracted.

Calculation of inhibition rate at clinical drug concentrations: Inhibition rates at clinically relevant blood concentrations were calculated using the formula: [1 - (luminescence value of drug-treated group - blank)/(control - blank)] × 100%, where the control group consisted of untreated organoids, and the blank accounted for background signal.

Clinical drug concentrations were derived from pharmacokinetic data reported in the literature: typical plasma levels of 5-FU (10 μM), oxaliplatin (5 μM), irinotecan (2 μM), and cetuximab (5×10^{-5} M) were used. Based on the inhibition rate at these concentrations, organoid sensitivity was categorized as follows: 0-25% (resistant), 26-50% (low sensitivity), 51-75% (moderate sensitivity), and 76-99% (high sensitivity). All measurements were performed in triplicate, and each experiment was repeated independently at least three times.

Sample quality score

The sample quality score was determined after preliminary culture. Samples were comprehensively scored based on the sampling method, time from sample removal to placement in preservation solution, sample quality, tissue cell proportion, cell viability, time to organoid formation, growth rate, and viability. Samples not meeting quality standards were not processed further.

Bias control

To minimize bias, only samples passing predefined quality standards were further cultivated. Standardized organoid processing and quality control assessments were employed to ensure consistency in PDO culture success rates.

Study size

A total of 16 CRC patients were recruited between September 2022 and September 2023. After applying inclusion criteria and conducting sample quality assessments using a standardized scoring system (**Table 1**), 11 specimens met the quality control (QC) criteria. Of these, 9 successfully yielded PDOs for subsequent drug sensitivity testing, resulting in a QC-adjusted success rate of 81.82% (9/11). The overall success rate based on all collected specimens was 56.25% (9/16) (**Figure 1**).

All 9 patients with successfully established PDOs completed clinical follow-up until July 31, 2024, with no loss to follow-up. The sample size was based on the estimated number of eligible CRC surgical patients during the study period and aligned with previous exploratory PDO studies of similar design [11, 12], which typically included 8-30 samples for investigating drug response and clinical correlations. Given the high cost, technical complexity, and time demands of organoid culture and drug screening, this sample size was deemed appropriate to assess feasibility and generate preliminary clinical insights.

Quantitative variables

Drug efficacy was evaluated through quantitative analysis of IC50 values and inhibition rates. A concentration gradient was set for each drug, and sensitivity was categorized as drug-resistant, low, moderate, or high, using the percentage of inhibition as the evaluation criterion.

Statistical methods

All statistical analyses were performed using GraphPad Prism 9.0 (GraphPad Software, San Diego, CA, USA). Data are presented as mean ± standard deviation (SD) from at least three independent experiments. For comparisons between two groups (e.g., drug-treated vs. control organoids), an unpaired two-tailed Student's t-test was used for normally distributed data, and the Mann-Whitney U test was used for non-normally distributed data. For multiple group comparisons (e.g., inhibition rates across different drugs), one-way analysis of variance (ANOVA) followed by Tukey's post hoc test was applied.

IC50 values were calculated by nonlinear regression using the log (inhibitor) vs. normalized response - variable slope model. Correlations between PDO inhibition rates and clinical outcomes were assessed using Spearman's rank correlation coefficient. The consistency of RAS mutation status between PDOs and patient tissues was analyzed using the chi-square test.

Table 1. Sample physical inspection scoring table

Item	Variable	Scoring criteria	Score
Sample information	Sampling method (A)	Surgical procedure	10
		Endoscope/puncture/biopsy	5
	Time from removal to placement in preservation solution (B)	< 10 mins	15
		10-20 mins	10
		> 20 mins	0
	Time of sample removal from body (C)	< 12 hours	10
		12-24 hours	5
		24-48 hours	0
	Sample mass/volume (D)	0.1-0.5 g or 50-200 ml	5
		< 0.1 g or 50 ml	0
	Proportion of tissue cells in the sample (E)	> 70%	10
		20%-70%	5
		< 20%	0
	Cell viability (F)	> 50%	10
		15%-50%	5
		< 15%	0
Proliferation capacity	Number of days to form organoids (G)	< 1 day	10
		≥ 2 days	5
	Growth rate of organoids (H)	Fast	15
		Moderate	10
		Slow	5
Other	Organoid viability (I)	> 50%	10
		15%-50%	5
		< 15%	0
	Temperature (J)	8-20°C	-5
		> 20°C	-15
	Validity of storage solution (K)	Expired	-10

Overall sample score (A+B+C+D+E+F+G+H+I+J+K).

A *P*-value < 0.05 was considered statistically significant.

Results

Construction of CRC organoids

Patient source and clinical characteristics: Basic patient information is summarized in **Table 2**. Samples were scored using an organoid sample scoring table. Those that failed the sample inspection were not cultured further (**Table 3**). Specifically, sample PDO-5 was discarded due to contamination, PDO-12 was discarded due to poor cell viability after tissue digestion, and PDO-10, PDO-13, and PDO-15 were abandoned due to low quality scores. Therefore, out of the 16 initial specimens, 11 passed the histological inspection. Samples PDO-7 and PDO-8 failed to culture due to continuous cell apoptosis and poor organoid formation, preventing completion of the drug sensitivity test. Nine organoids were successfully cultured, yielding a success rate of 81.82%, consistent with previous reports [13, 14].

Morphological characteristics of organoids

Organoid morphology was observed under a light microscope. On day 1, a few scattered cells were visible, showing rounding and healing, indicating good cell viability. By day 3, the organoid diameter had increased, with some exceeding 50 μm. By day 14, organoids displayed 3D spherical structures, ranging from 100 to 200 μm in diameter. CRC organoids exhibited both thin-walled and thick-walled cystic structures, and no solid spherical structures were observed, as reported in previous studies [11]. This could be due to the limited number of cases studied.

The morphology of CRC organoids varied across patients. PDO1, PDO2, PDO3, PDO4, and

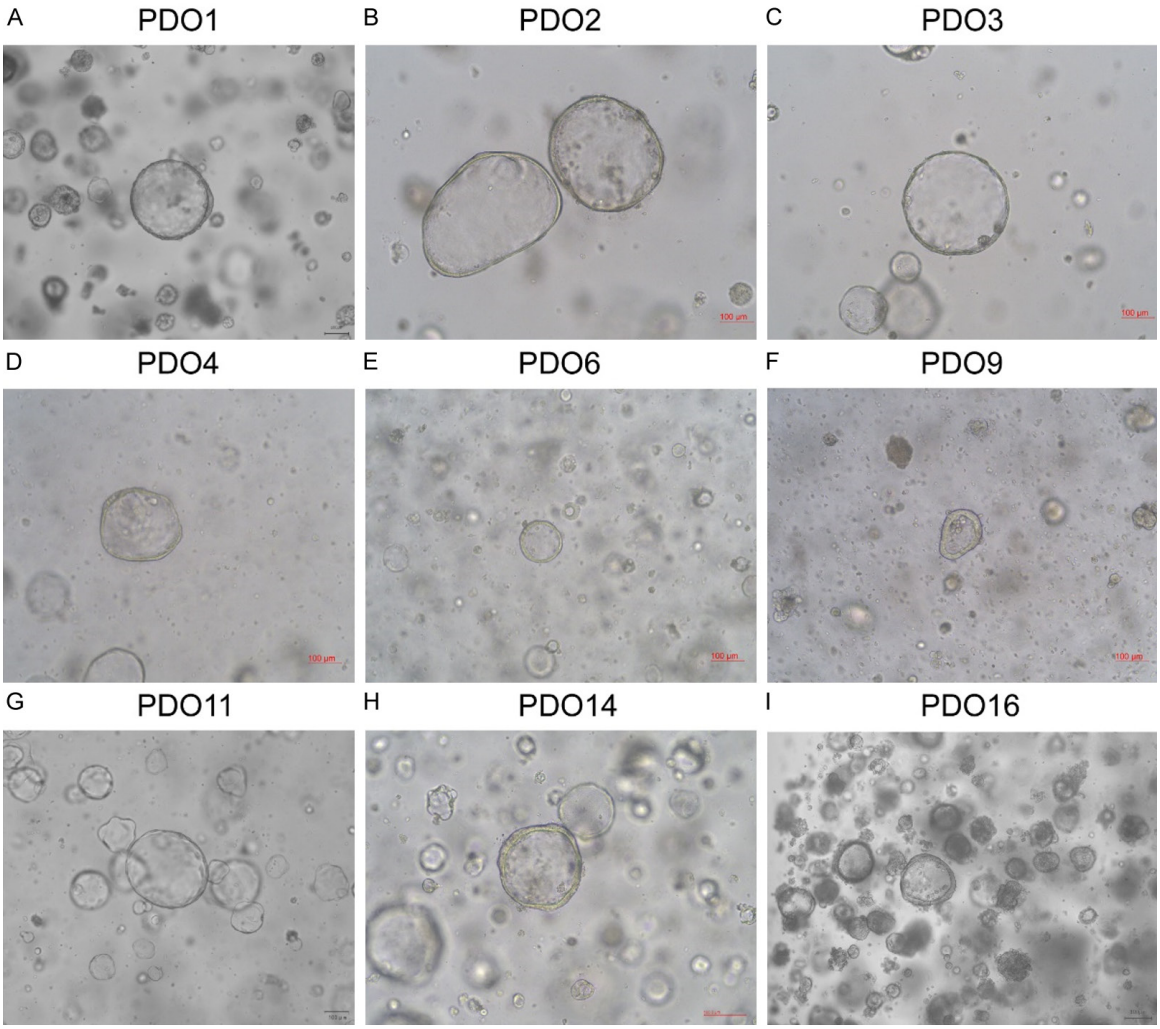

Figure 1. Morphological characteristics of nine PDOs. A-I. Bright-field microscopic images of PD001, PD002, PD003, PD004, PD006, PD009, PD011, PD014, and PD016, respectively. The organoids exhibit diverse morphologies and sizes, reflecting inter-patient heterogeneity. Scale bar: 100 μm.

PD011 displayed thin-walled cystic structures, while PD06, PD09, PD014, and PD016 showed thick-walled cystic structures.

Drug sensitivity test of organoids

To assess the in vitro drug response of CRC organoids and evaluate their sensitivity to chemotherapeutic and targeted drugs, we performed drug sensitivity tests on the nine successfully cultured CRC organoids. According to international and domestic guidelines, five chemotherapeutic agents and one targeted drug commonly used in CRC treatment were selected: irinotecan, oxaliplatin, 5-FU, leucovorin, and trifluridine (TAS-102). Drug concentrations were set in a gradient from 100 to 0.0001 μM to calculate IC50 values. The IC50 values for each organoid in response to various drugs are summarized in **Table 4**. A slash in the table indicates that the data could not be fitted.

As shown in the drug dose-response graphs (**Figures 2** and **3**), there were significant differences in drug responses between different organoids and also varying responses of the same organoid to different drugs. Compared to other drugs, all organoids showed a better drug response to irinotecan. For raltitrexed, the cell activity of PD01, PD02, PD04, PD09, PD011, PD014 and PD016 organoids hardly changed with varying drug concentrations. Only PD02 exhibited a favorable response to cetuximab,

Table 2. Basic information about the patient

Number	Gender	Age	Tumor location	Histological grade	T	N	M	Stage	Vascular invasion	Nerve invasion	Tumor budding	KRAS	NRAS	BRAF
PD01	Male	54	Sigmoid colon	Well differentiated	T3	N2b	M1a (Liver)	IVA	-	-	-	wt	wt	wt
PD02	Male	71	Rectum	Moderately differentiated	T3	N1	M0	IIIB	+	-	-	wt	wt	wt
PD03	Female	56	Sigmoid colon	Moderately differentiated	T3	N1	M0	IIIB	-	-	-	mut	wt	wt
PD04	Male	69	Sigmoid colon	Poorly differentiated	T3	N1	M0	IIIB	+	+	-	wt	wt	wt
PD05	Male	60	Rectum	Moderately differentiated	T3	N1	M1a (Liver)	IVA	-	-	-	mut	wt	wt
PD06	Male	76	Sigmoid colon	Poorly differentiated	T3	N1	M0	IIIB	+	+	-	mut	wt	wt
PD07	Female	70	Rectum	Moderately differentiated	T3	N1	M1a (Liver)	IVA	-	-	-	wt	wt	wt
PD08	Male	54	Rectum	Poorly differentiated	T3	N2a	M1a (Lung)	IVA	-	-	-	wt	mut	wt
PD09	Female	70	Sigmoid colon	Moderately differentiated	T3	N1	M0	IIIB	+	+	-	wt	wt	wt
PD010	Female	69	Descending colon	Moderately differentiated	T1	N2a	M0	IIIA	-	-	-	wt	wt	wt
PD011	Male	66	Rectum	Poorly differentiated	T3	N2a	M0	IIIB	-	+	+	mut	wt	wt
PD012	Female	44	sigmoid colon	Well differentiated	T3	N1	M1a (Liver)	IVA	-	-	+	wt	wt	wt
PD013	Female	74	Sigmoid colon	Well differentiated	T2	N1	M1a (Lung)	IVA	-	-	+	wt	wt	wt
PD014	Male	40	Rectum	Poorly differentiated	T2	N1	M0	IIIA	+	-	-	wt	mut	wt
PD015	Male	53	Rectum	Moderately differentiated	T3	N1	M1a (Liver)	IVA	-	-	-	wt	wt	wt
PD016	Female	66	Descending colon	Poorly differentiated	T4b	N1	M0	IIIC	+	-	-	mut	wt	wt

Table 3. Sample inspection scores and cultivation results

Number	Quality score	Sample inspection	Cultivation results
PD01	65	Qualified	Successful
PD02	45	Qualified	Successful
PD03	65	Qualified	Successful
PD04	55	Qualified	Successful
PD05	50	Unqualified	Failure
PD06	50	Qualified	Successful
PD07	70	Qualified	Failure
PD08	65	Qualified	Failure
PD09	65	Qualified	Successful
PD010	25	Unqualified	Failure
PD011	40	Qualified	Successful
PD012	60	Unqualified	Failure
PD013	25	Unqualified	Failure
PD014	65	Qualified	Successful
PD015	25	Unqualified	Failure
PD016	55	Qualified	Successful

while the remaining organoids showed poorer responses.

We next evaluated the inhibition rates of organoids at clinically relevant blood concentrations. The inhibition rates of each organoid to each drug at blood concentrations are shown in **Figure 4**.

PD01 was moderately sensitive to oxaliplatin (inhibition rate of 61.59%) and irinotecan, but resistant to other drugs.

PD02 was extremely sensitive to cetuximab (inhibition rate of 86.2%), moderately sensitive to trifluridine (56.87%), oxaliplatin (56.87%), 5-FU (56.87%), and irinotecan (32.95%).

PD03 showed moderate sensitivity to oxaliplatin (32.95%) and raltitrexed (28.18%).

PD04 exhibited moderate sensitivity to trifluridine (27.26%) and cetuximab (32.09%).

PD06 was moderately sensitive to oxaliplatin, 5-FU, and cetuximab, with inhibition rates of 40.75%, 29.46%, and 34.10%, respectively.

PD09 was lowly sensitive to oxaliplatin (33.57%), irinotecan (35.65%), and cetuximab (32.64%).

PD011 was only lowly sensitive to oxaliplatin, with an inhibition rate of 48.81%.

PD014 was moderately sensitive to irinotecan (63.18%) and moderately sensitive to oxaliplatin (42.26%) and trifluridine (26.31%).

Patient PD01 presented with liver metastases and intestinal obstruction at the time of initial diagnosis. After undergoing surgery for colon cancer, he received 4 cycles of FOLFOXIRI + Cetuximab. Follow-up CT scans showed a reduction in liver metastases, leading to resection of the liver metastases. Subsequently, he switched to CapeOx + Cetuximab for 6 cycles, but new liver and abdominal metastases appeared. The progression-free survival (PFS) was 199 days. After 5 additional cycles of FOLFOXIRI + Cetuximab, the metastases shrank again. However, upon switching to CapeOx + Cetuximab for 4 more cycles, the tumor progressed once more. The patient opted to discontinue chemotherapy and switched to traditional Chinese medicine, refusing further follow-up.

PD016 underwent chemotherapy with the FOLFOX regimen after surgery and was diagnosed with advanced lung cancer on June 10, 2023. Since then, he has not been regularly followed up, and pelvic metastases were discovered on April 17, 2024. The patient, in poor health, declined radiotherapy and continued with only maintenance treatment using capecitabine and bevacizumab. The remaining seven patients all received chemotherapy with the FOLFOX regimen after surgery and have been followed up for 15-18 months without tumor progression.

Despite many patient organoids showing weak sensitivity to chemotherapy, clinical efficacy remained favorable. In patients with RAS gene mutations, organoid responses to Cetuximab treatment were all insensitive. PD01, a RAS wild-type patient, developed resistance to Cetuximab, consistent with clinical outcomes. This suggests that organoids may be valuable in predicting the efficacy of CRC treatment.

Discussion

Current CRC treatment strategies are far from optimal, as primary drug resistance limits ther-

Table 4. Organoid drug IC50 values (μM)

IC50	Oxaliplatin	5-FUFu	Irinotecan	Trifluridine	Retapamulin	Cetuximab
PD01	26.34	/	1.050	102.7	/	/
PD02	18.03	90.3	0.088	0.084	/	0.00035
PD03	106	482.3	12.98	54.39	425.7	/
PD04	328.3	4757	2.56	1945	/	/
PD06	69.16	62.14	3.98	280.1	3935	/
PD09	287.2	/	0.23	2848	/	/
PD011	15.12	92.48	0.94	/	6805	18.68
PD014	206.4	220.9	0.14	155.6	/	/
PD016	22.28	173.4	0.028	387.9	0.0584	0.00203

apeutic efficacy. Various models have been developed to predict drug efficacy. Wong et al. analyzed 406,038 drug screening clinical trials from January 1, 2000, to October 31, 2015, and found that the overall success rate of Phase I-III drug trials was only 13.8%, with cancer drug trials showing a mere 3.4% success rate [15]. A significant number of 2D cultured cell line screenings for anti-cancer drugs have failed in clinical trials [16, 17]. Genetic testing using next-generation sequencing technology has become a common tool for personalized cancer treatment. Cetuximab is clinically used to treat CRC with confirmed KRAS/NRAS wild-type via genetic testing [18]. Drugs targeting the epidermal growth factor receptor (EGFR), like cetuximab, significantly extend PFS and overall survival in advanced CRC patients. However, recent clinical data show that not all RAS wild-type CRC patients benefit from Cetuximab. For example, a randomized Phase III trial reported an objective response rate of 69.1% with Cetuximab plus FOLFIRI, compared to 42.3% with FOLFIRI alone in RAS/BRAF wild-type metastatic CRC patients [19]. Additionally, exploratory analysis of FOLFOXIRI plus Cetuximab showed varied ORR, PFS, and OS, highlighting heterogeneous sensitivity to Cetuximab even among RAS wild-type patients [20]. Furthermore, many patients develop resistance after 3-12 months of Cetuximab treatment [21, 22]. Hence, there is an urgent need to develop in vitro models capable of accurately predicting drug efficacy. In this study, we present a successful method for constructing CRC organoids that closely resemble the original patient tumors.

The success rate of organoid culture for CRC varies across different studies. Ganesh et al. obtained 84 rectal cancer specimens with a 77% success rate [23], while Yao et al. achieved an 85.7% success rate with 112 rectal cancer biopsies [24]. Ooft et al. achieved a 63% success rate with 63 CRC specimens [12], and Mo et al. reported 86.11% and 75% success rates for CRC primary lesions and liver metastases, respectively [11]. Bruun et al. obtained 75 specimens from 29 patients, with a success rate of 52% [25]. In our study, 16 patients were selected, and 9 organoids were successfully cultured, yielding a success rate of 56.25%. After scoring the samples post-culture for quality, 11 samples passed the quality criteria, and 9 organoids were successfully cultured, resulting in an 81.82% success rate. This aligns with previous reports. Standardizing the specimen collection process-such as choosing appropriately sized tumor samples, ensuring purity, and minimizing bacterial contamination-could improve organoid culture success rates [26]. Additionally, factors like aseptic handling and careful monitoring of organoid growth during culture are crucial for improving culture outcomes.

As a promising alternative to traditional cell line cultures and PDX models, organoid models offer significant advantages, including cost-effectiveness and a closer replication of in vivo tumor characteristics [27]. PDOs have proven to be reliable predictors of drug response in various cancers, including breast cancer [28], lung cancer, gastric cancer, pancreatic cancer, and ovarian cancer [29-32]. Mo et al. demonstrated that organoids can predict chemotherapy efficacy in advanced CRC [11], although their study did not include targeted therapy drugs. In this study, we successfully established CRC organoids and performed drug sensitivity test-

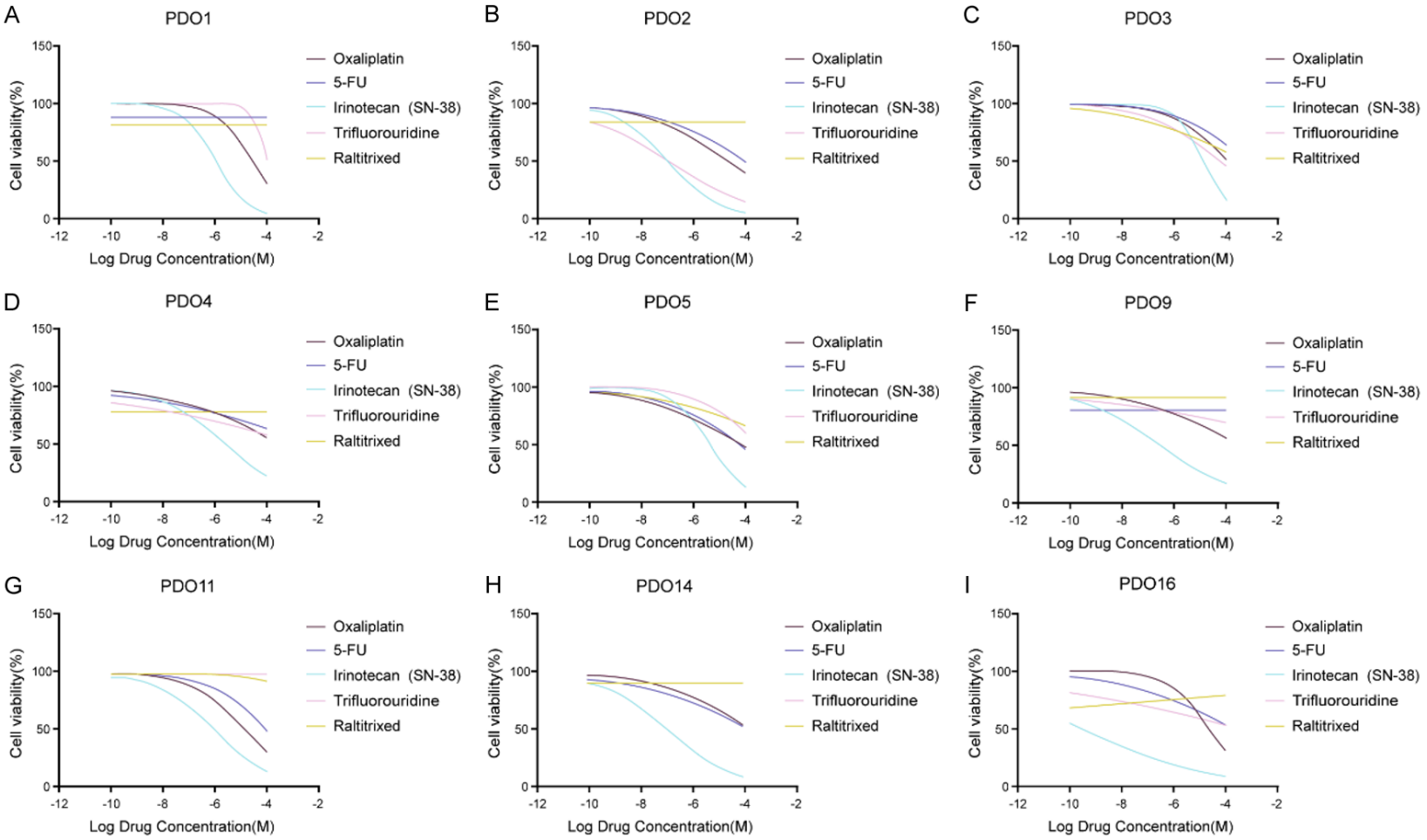

Figure 2. Drug response curves of colorectal cancer PDOs treated with five chemotherapeutic agents. (A-I) Dose-response curves for PDO01 (A), PDO02 (B), PDO03 (C), PDO04 (D), PDO06 (E), PDO09 (F), PDO11 (G), PDO14 (H), and PDO16 (I) treated with oxaliplatin, 5-fluorouracil (5-FU), irinotecan (SN-38), trifluridine, and raltitrexed. Cell viability was measured after 72 hours of drug exposure. Each curve represents the mean cell viability at varying concentrations of each drug, illustrating inter-patient heterogeneity in drug sensitivity.

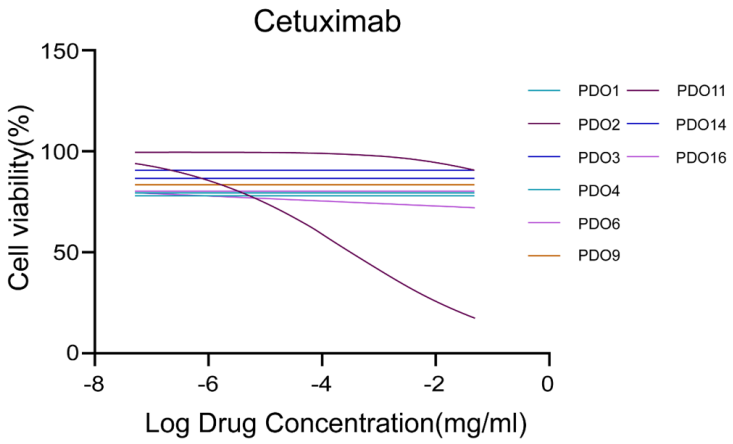

Figure 3. Cetuximab sensitivity among PDOs. Dose-response curves of Cetuximab treatment across 9 colorectal cancer PDO lines (PDO01, PDO02, PDO03, PDO04, PDO06, PDO09, PDO11, PDO14, and PDO16). Most PDOs exhibited resistance to Cetuximab with minimal decrease in cell viability, whereas PDO02 showed a marked dose-dependent response, indicating selective sensitivity.

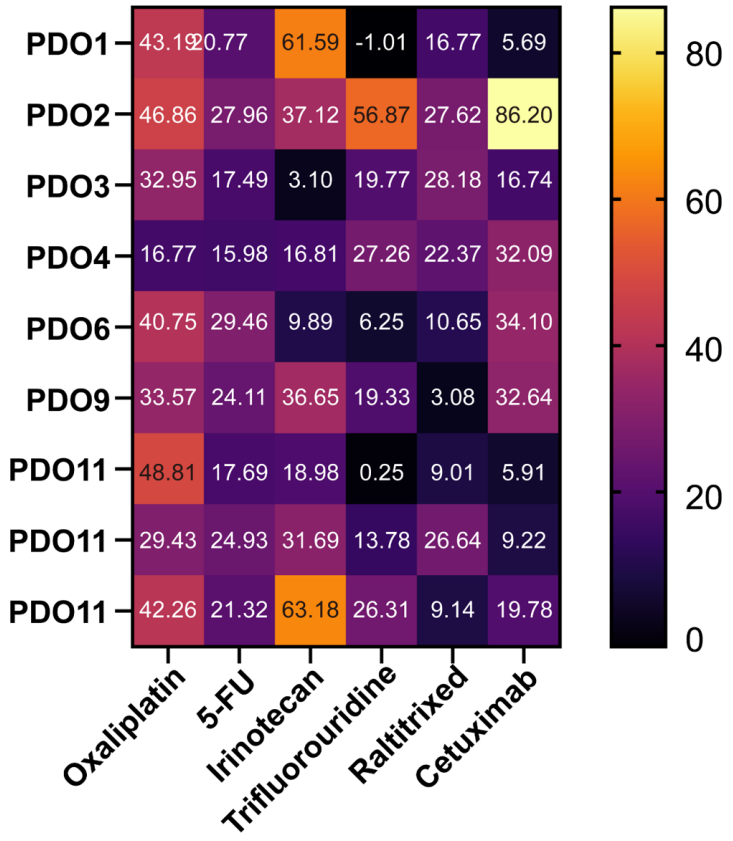

Figure 4. Inhibition rate of each drug across PDOs at physiological blood concentrations. Heatmap illustrating the percentage inhibition rates of six chemotherapeutic agents (Oxaliplatin, 5-FU, Irinotecan, Trifluridine, Raltitrexed, and Cetuximab) in individual colorectal cancer PDO lines. Each value represents the average inhibition rate (%) at clinically relevant drug concentrations. Notably, PDO2 exhibited high sensitivity to Cetuximab (86.20%), while other PDOs demonstrated heterogeneous responses across different drugs.

ing using five chemotherapeutic agents and one targeted drug commonly used in CRC treatment: irinotecan, oxaliplatin, 5-FU, leucovorin, trifluridine (tas-102), and cetuximab.

In addition to calculating the inhibition rate of drugs at blood concentrations, we also determined the IC50 values for various organoids exposed to different drugs, comparing these values against clinically relevant blood concentrations as a benchmark for drug response evaluation. However, for certain organoids, drug responses did not change significantly with varying concentrations, preventing accurate IC50 calculation. We hypothesize that this may be due to intratumoral heterogeneity. Despite this, the study revealed differences in drug sensitivity across organoids, specifically to Irinotecan, Oxaliplatin, 5-Fu, Raltitrexed, Trifluridine, and Cetuximab. Clinical follow-up showed that even when patient organoids were weakly sensitive to Oxaliplatin and 5-FU, favorable therapeutic outcomes were observed.

In line with previous findings, our cetuximab susceptibility test demonstrated resistance in organoids from patients with RAS mutations. Interestingly, one RAS wild-type patient (PDO1) exhibited resistance to cetuximab, which was validated by clinical follow-up. PDO1 showed low sensitivity to Oxaliplatin, moderate sensitivity to Irinotecan, and resistance to other drugs. During clinical treatment, liver metastases shrank after FOLFOXIRI + Cetuximab but progressed after switching to CapeOx + Cetuximab, aligning with the organoid drug sensitivity test results. This suggests that CRC organoid drug responses are consistent with clinical outcomes and that organ-

oid models hold potential for predicting patient-specific drug sensitivity.

Limitations

Despite the promising results, this study has several limitations. First, CRC treatment is often based on combination therapies. In this study, we tested individual drugs, which may not fully capture the interactions between them. For example, the combination of 5-FU and oxaliplatin enhances the efficacy of both agents. A more comprehensive approach that includes combination therapy testing would be beneficial. Additionally, due to the short follow-up period, many patients have not experienced significant events like tumor recurrence, which means further long-term follow-up is needed. Lastly, expanding the sample size would strengthen the conclusions drawn from this study.

Conclusion

The construction of CRC organoid models has demonstrated a viable success rate, and the use of sample quality testing can further improve the success rate of organoid culture. CRC organoids can be stably cultured, passaged, and maintain tissue morphology before and after cryopreservation and resuscitation. Drug sensitivity test results from organoid models align well with clinical outcomes, reflecting the drug sensitivity of individual patients. These findings provide valuable guidance for clinical CRC treatment, supporting the development of personalized and precision treatment strategies. Further large-scale research and validation are warranted to optimize the application of organoid models in clinical practice.

Acknowledgements

This study was supported by Wenzhou Municipal Science and Technology Bureau (No. Y2020145 to Yiwang Hu) and the scientific research project of Shanghai Cancer Prevention and Cancer Career Development Foundation (Contract (2023) 1941 of the First Hospital of Wenzhou Medical University).

Disclosure of conflict of interest

None.

Address correspondence to: Yifei Pan, Department of Colorectal and Anal Surgery, The First Affiliated Hospital of Wenzhou Medical University, Nanbaixiang Campus, Wenzhou 325000, Zhejiang, China. E-mail: Clocklover@126.com

References

[1] Sung H, Ferlay J, Siegel RL, Laversanne M, Soerjomataram I, Jemal A and Bray F. Global cancer statistics 2020: GLOBOCAN estimates of incidence and mortality worldwide for 36 cancers in 185 countries. CA Cancer J Clin 2021; 71: 209-249.

[2] Siegel RL, Wagle NS, Cercek A, Smith RA and Jemal A. Colorectal cancer statistics, 2023. CA Cancer J Clin 2023; 73: 233-254.

[3] Shaham SH, Vij P and Tripathi MK. Advances in targeted and chemotherapeutic strategies for colorectal cancer: current insights and future directions. Biomedicines 2025; 13: 642.

[4] Stintzing S, Heinrich K, Tougeron D, Modest DP, Schwaner I, Eucker J, Pihusch R, Stauch M, Kaiser F, Kahl C, Karthaus M, Müller C, Burkart C, Reinacher-Schick A, Kasper-Virchow S, Fischer von Weikersthal L, Krammer-Steiner B, Prager GW, Taieb J and Heinemann V. FOLFOXIRI plus cetuximab or bevacizumab as first-line treatment of BRAF(V600E)-mutant metastatic colorectal cancer: the randomized phase II FIRE-4.5 (AIO KRK0116) study. J Clin Oncol 2023; 41: 4143-4153.

[5] Ciracì P, Studiale V, Taravella A, Antoniotti C and Cremolini C. Late-line options for patients with metastatic colorectal cancer: a review and evidence-based algorithm. Nat Rev Clin Oncol 2025; 22: 28-45.

[6] Abuwatfa WH, Pitt WG and Husseini GA. Scaffold-based 3D cell culture models in cancer research. J Biomed Sci 2024; 31: 7.

[7] Xu S, Yin SY, Bie ZX, Li YM, Qi J, Ma YD, Wang Z, Xi JJ and Li XG. Personalized drug screening of patient-derived tumor-like cell clusters based on specimens obtained from percutaneous transthoracic needle biopsy in patients with lung malignancy: a real-world study. BMC Cancer 2025; 25: 649.

[8] Zanella ER, Grassi E and Trusolino L. Towards precision oncology with patient-derived xenografts. Nat Rev Clin Oncol 2022; 19: 719-732.

[9] Clevers H. Modeling development and disease with organoids. Cell 2016; 165: 1586-1597.

[10] Tang XY, Wu S, Wang D, Chu C, Hong Y, Tao M, Hu H, Xu M, Guo X and Liu Y. Human organoids in basic research and clinical applications. Signal Transduct Target Ther 2022; 7: 168.

[11] Mo SB, Tang PY, Luo WQ, Zhang L, Li YQ, Hu X, Ma XJ, Chen YK, Bao YC, He XF, Fu GX, Xu XY, Rao XX, Li XM, Guan RY, Chen SZ, Deng Y, Lv T,

Mu PY, Zheng Q, Wang SM, Liu FQ, Li YW, Sheng WQ, Huang D, Hu C, Gao JJ, Zhang Z, Cai SJ, Clevers H, Peng JJ and Hua GQ. Patient-derived organoids from colorectal cancer with paired liver metastasis reveal tumor heterogeneity and predict response to chemotherapy. Adv Sci (Weinh) 2022; 9: e2204097.

[12] Ooft SN, Weeber F, Dijkstra KK, McLean CM, Kaing S, van Werkhoven E, Schipper L, Hoes L, Vis DJ, van de Haar J, Prevoo W, Snaebjornsson P, van der Velden D, Klein M, Chalabi M, Boot H, van Leerdam M, Bloemendal HJ, Beerepoot LV, Wessels L, Cuppen E, Clevers H and Voest EE. Patient-derived organoids can predict response to chemotherapy in metastatic colorectal cancer patients. Sci Transl Med 2019; 11: eaay2574.

[13] Lau HCH, Kranenburg O, Xiao HP and Yu J. Organoid models of gastrointestinal cancers in basic and translational research. Nat Rev Gastroenterol Hepatol 2020; 17: 203-222.

[14] Vlachogiannis G, Hedayat S, Vatsiou A, Jamin Y, Fernández-Mateos J, Khan K, Lampis A, Eason K, Huntingford I, Burke R, Rata M, Koh DM, Tunariu N, Collins D, Hulkki-Wilson S, Ragulan C, Spiteri I, Moorcraft SY, Chau I, Rao S, Watkins D, Fotiadis N, Bali M, Darvish-Damavandi M, Lote H, Eltahir Z, Smyth EC, Begum R, Clarke PA, Hahne JC, Dowsett M, de Bono J, Workman P, Sadanandam A, Fassan M, Sansom OJ, Eccles S, Starling N, Braconi C, Sottoriva A, Robinson SP, Cunningham D and Valeri N. Patient-derived organoids model treatment response of metastatic gastrointestinal cancers. Science 2018; 359: 920-926.

[15] Wong CH, Siah KW and Lo AW. Estimation of clinical trial success rates and related parameters (vol 20, pg 273, 2019). Biostatistics 2019; 20: 366.

[16] Foglizzo V, Cocco E and Marchiò S. Advanced cellular models for preclinical drug testing: from 2D cultures to organ-on-a-chip technology. Cancers (Basel) 2022; 14: 3692.

[17] Badea MA, Balas M, Ionita D and Dinischiotu A. Carbon nanotubes conjugated with cisplatin activate different apoptosis signaling pathways in 2D and 3D-spheroid triple-negative breast cancer cell cultures: a comparative study. Arch Toxicol 2024; 98: 2843-2866.

[18] Weiss L, Stintzing S, Stahler A, Benedikt Westphalen C, von Weikersthal LF, Decker T, Kiani A, Vehling-Kaiser U, Al-Batran SE, Heintges T, Lerchenmüller CA, Kahl C, Seipelt G, Kullmann F, Heinrich K, Holch JW, Alig A, Jung A, Modest DP and Heinemann V. Molecular hyperselection for optimal choice of first-line targeted therapy independent of primary tumor sidedness: an exploratory analysis of the randomized FIRE-3 study performed in RAS wild-type metastatic colorectal cancer. Eur J Cancer 2025; 221: 115399.

[19] Shi Y, Ba Y, Wang J, Xiong J, Gu K, Chen Y, Zheng Z, Wang Z, Guo W, Cheng Y, Yin X, Liu Y, Bai Y, Li E, Li Q, Zhu L, Li W, Jiang D, He J, Chen J, Sun J and Hou S. First-line treatment of anti-EGFR monoclonal antibody cetuximab β plus FOLFIRI versus FOLFIRI alone in Chinese patients with RAS/BRAF wild-type metastatic colorectal cancer: a randomized, phase 3 trial. Signal Transduct Target Ther 2025; 10: 147.

[20] Shiozawa M, Sunakawa Y, Watanabe T, Ota H, Yasui H, Yabuno T, Tei M, Kochi M, Manaka D, Ohori H, Yamaguchi T, Sagawa T, Kotaka M, Kubota Y, Sekikawa T, Nakamura M, Takeuchi M, Ichikawa W, Fujii M and Tsuji A. Modified FOLFOXIRI plus cetuximab versus bevacizumab in RAS wild-type metastatic colorectal cancer: a randomized phase II DEEPER trial. Nat Commun 2024; 15: 10217.

[21] Ríos-Hoyo A, Monzonís X, Vidal J, Linares J and Montagut C. Unveiling acquired resistance to anti-EGFR therapies in colorectal cancer: a long and winding road. Front Pharmacol 2024; 15: 1398419.

[22] Bianchini S, Bovio F, Negri S, Guzzo F, Forcella M and Fusi P. Gratiola officinalis alcoholic extract targets warburg effect, apoptosis and cell cycle progression in colorectal cancer cell lines. Int J Mol Sci 2025; 26: 2220.

[23] Ganesh K, Wu C, O'Rourke KP, Szeglin BC, Zheng Y, Sauvé CG, Adileh M, Wasserman I, Marco MR, Kim AS, Shady M, Sanchez-Vega F, Karthaus WR, Won HH, Choi SH, Pelossof R, Barlas A, Ntiamoah P, Pappou E, Elghouayel A, Strong JS, Chen CT, Harris JW, Weiser MR, Nash GM, Guillem JG, Wei IH, Kolesnick RN, Veeraraghavan H, Ortiz EJ, Petkovska I, Cercek A, Manova-Todorova KO, Saltz LB, Lavery JA, DeMatteo RP, Massagué J, Paty PB, Yaeger R, Chen X, Patil S, Clevers H, Berger MF, Lowe SW, Shia J, Romesser PB, Dow LE, Garcia-Aguilar J, Sawyers CL and Smith JJ. A rectal cancer organoid platform to study individual responses to chemoradiation. Nat Med 2019; 25: 1607-1614.

[24] Yao Y, Xu X, Yang L, Zhu J, Wan J, Shen L, Xia F, Fu G, Deng Y, Pan M, Guo Q, Gao X, Li Y, Rao X, Zhou Y, Liang L, Wang Y, Zhang J, Zhang H, Li G, Zhang L, Peng J, Cai S, Hu C, Gao J, Clevers H, Zhang Z and Hua G. Patient-derived organoids predict chemoradiation responses of locally advanced rectal cancer. Cell Stem Cell 2020; 26: 17-26, e6.

[25] Bruun J, Kryeziu K, Eide PW, Moosavi SH, Eilertsen IA, Langerud J, Rosok B, Totland MZ, Brunsell TH, Pellinen T, Saarela J, Bergsland CH, Palmer HG, Brudvik KW, Guren T, Dienstmann R, Guren MG, Nesbakken A,

Bjornbeth BA, Sveen A and Lothe RA. Patient-derived organoids from multiple colorectal cancer liver metastases reveal moderate intra-patient pharmacotranscriptomic heterogeneity. Clin Cancer Res 2020; 26: 4107-4119.

[26] Zhou C, Wu Y, Wang Z, Liu Y, Yu J, Wang W, Chen S, Wu W, Wang J, Qian G and He A. Standardization of organoid culture in cancer research. Cancer Med 2023; 12: 14375-14386.

[27] Xiao Y, Li Y, Jing X, Weng L, Liu X, Liu Q and Chen K. Organoid models in oncology: advancing precision cancer therapy and vaccine development. Cancer Biol Med 2025; 22: 903-927.

[28] Shi Y, Guan Z, Cai G, Nie Y, Zhang C, Luo W and Liu J. Patient-derived organoids: a promising tool for breast cancer research. Front Oncol 2024; 14: 1350935.

[29] Wang HM, Zhang CY, Peng KC, Chen ZX, Su JW, Li YF, Li WF, Gao QY, Zhang SL, Chen YQ, Zhou Q, Xu C, Xu CR, Wang Z, Su J, Yan HH, Zhang XC, Chen HJ, Wu YL and Yang JJ. Using patient-derived organoids to predict locally advanced or metastatic lung cancer tumor response: a real-world study. Cell Rep Med 2023; 4: 100911.

[30] Zu M, Hao X, Ning J, Zhou X, Gong Y, Lang Y, Xu W, Zhang J and Ding S. Patient-derived organoid culture of gastric cancer for disease modeling and drug sensitivity testing. Biomed Pharmacother 2023; 163: 114751.

[31] Demyan L, Habowski AN, Plenker D, King DA, Standring OJ, Tsang C, St Surin L, Rishi A, Crawford JM, Boyd J, Pasha SA, Patel H, Galluzzo Z, Metz C, Gregersen PK, Fox S, Valente C, Abadali S, Matadial-Ragoo S, DePeralta DK, Deutsch GB, Herman JM, Talamini MA, Tuveson DA and Weiss MJ. Pancreatic cancer patient-derived organoids can predict response to neoadjuvant chemotherapy. Ann Surg 2022; 276: 450-462.

[32] Fashemi BE, van Biljon L, Rodriguez J, Graham O, Mullen M and Khabele D. Ovarian cancer patient-derived organoid models for pre-clinical drug testing. J Vis Exp 2023; 10.3791/65068.